SINTERING AND MECHANICAL PROPERTIES OF ALUMINA-YTTRIUM ALUMINATE COMPOSITES

A THESIS SUBMITTED IN PARTIAL FULFILMENT
OF THE REQUIREMENT FOR THE DEGREE OF

Master of Technology

in

INDUSTRIAL CERAMICS

BY

SUDHANSHU RANJAN

213CR2133

DEPARTMENT OF CERAMIC ENGINEERING
NATIONAL INSTITUTE OF TECHNOLOGY
Rourkela

MAY 2015

CERTIFICATE

This is to certify that the thesis entitled "**SINTERING AND MECHANICAL PROPERTIES OF ALUMINA-YTTRIUM ALUMINATE COMPOSITES**" submitted by **Mr. SUDHANSHU RANJAN** (213CR2133) in partial fulfilment of the requirement for the award of **MASTER OF TECHNOLOGY** degree in **INDUSTRIAL CERAMIC ENGINEERING** at the **NATIONAL INSTITUTE OF TECHNOLOGY**, **ROURKELA** is an authentic work carried out by him under my supervision and guidance.To the best of my knowledge, the matter embodied in the thesis has not been submitted to any other University/Institute for the award of any Degree or Diploma.

Date

S.BHATTACHARYYA
Dept. of Ceramic Engineering
National Institute of Technology
Rourkela-769008

ACKNOWLEDGEMENT

I wish to express my deep sense of gratitude and indebtedness to **Prof. S. Bhattacharyya,** Department of Ceramic Engineering, N.I.T Rourkela for assigning me the project "**SINTERING AND MECHANICAL PROPERTIES OF ALUMINA-YTTRIUM ALUMINATE COMPOSITES**" and for his inspiring guidance, constructive criticism and valuable suggestion throughout this project work.

I am very thankful to **Prof. S. K. Pratihar**, Head of The Department, for his cooperation. It would haven't been possible for me to bring out this project report without his help and constant encouragement. I would like to express to our **Prof. J. Bera, Prof. R. Sarkar** for their valuable suggestions and encouragements at various stages of the work.

I am also thankful to research scholars in Department of Ceramic Engineering for providing all joyful environments in the lab and helping me throughout this project. I would also take this opportunity to express my gratitude to **Bapi Sir** and **Arvind Kumar** Sir for their help, and lastly I am thankful to my parents and friends for their constant support.

SUDHANSHU RANJAN

213CR2133

INDEX

CHAPTER NO.	TITLE	PAGE NO.
	ABSTRACT	i
	LIST OF TABLES	ii
	LIST OF FIGURES	iii
1	INTRODUCTION	1
2	LITERATURE REVIEW	4
3	EXPERIMENTAL WORK	10
3.1	Powder Processing	11
3.1.1	Synthesis of Yttrium Nitrate	11
3.1.2	Estimation of Yttrium Nitrate solution	11
3.1.3	Preparation of Al_2O_3 –$Y(NO_3)_2$ mix and calcination	12
3.1.4	Compaction and Sintering	12
3.1.5	Processing of Al_2O_3-YAG Composites	13
3.2	Flow sheet of processing of the Al_2O_3-YAG Composites.	13
3.3	Characterization	14
3.3.1	Thermal decomposition behaviour of Al_2O_3 Yttrium Nitrate powder mix	14
3.3.2	XRD	14
3.3.3	Bulk Density and Apparent Porosity	14

3.3.4	Vickers Hardness	14
3.3.5	Flexural Strength	15
3.3.6	Fracture Toughness	16
3.3.7	Microstructure of Sintered Specimens	17
4	RESULTS AND DISCUSSIONS	18
4.1	Decomposition behaviour of Yttrium Nitrate and Crystallization of Yttrium Aluminate	19
4.2	Phase evolution in the calcined Al_2O_3-Y_2O_3 powder	20
4.2.1	Phase Evolution in Al_2O_3-40 mol % Y_2O_3	21
4.2.2	Phase Evolution in Al_2O_3-50 mol % Y_2O_3	21
4.2.3	Phase Evolution in Al_2O_3-60 mol % Y_2O_3	22
4.3	Phase analysis of sintered Al_2O_3- Yttrium Aluminate Composites	22
4.4	Bulk Density and Relative Density of Sintered Alumina as a function of Yttrium Aluminate of Composites	25
4.5	Apparent Porosity of Sintered Alumina as a function of Yttrium Aluminate of Composites	26
4.6	Hardness of Sintered Alumina as a function of Yttrium Aluminate of Composites	27
4.7	Flexural Strength of sintered Alumina as a function of Yttrium Aluminate of Composites	27
4.8	Fracture Toughness of sintered Alumina as a function of Yttrium Aluminate of Composites	28

4.9	Microstructure of Sintered Specimen Alumina-YAG Composites	29
4.10	Microstructure of indented samples of Alumina-YAG Composites	29
5	CONCLUSIONS	31
	REFERENCES	33

ABSTRACT

Yttrium Aluminate (having different mole percent of Y_2O_3) were prepared by mixing of Al_2O_3 and $Y(NO_3)_2.6H_2O$ and calcination of powder at 1400^oC. The calcined Yttrium Aluminate powder was added to Aluminain different volume fractions (5, 10, 15 and 20 vol%), compacted and sintered at 1650^oC. The sintered sample had a relative density (82-90 % of theoretical). The sintered samples were characterised by bulk density, apparent porosity, hardness, strength, toughness and microstructure. The fracture toughness as measured by Indentation Strength in Bending(ISB) method was 2.4 MPa√m for pure Alumina and it increased to 4.21 MPa√m at 20 vol% Yttrium Aluminate addition. Microstructure showed that the Yttrium Aluminate was inhomogeneously distributed in the Alumina matrix. The crack path of the indented samples indicates that crack bowing takes place in Alumina–Yttrium Aluminate samples. It is concluded that proper densification of the composites could possibly further increase the toughness and strength.

LIST OF TABLES

S.no	Title	Page no
4.1	Relative Fraction of Al_2O_3 and YAG in the Sintered Samples of Alumina- Yttrium Aluminate Composites	25
4.2	Relative density of Yttrium Aluminate phases in alumina	25
4.3	Fracture toughness of sintered sample at 1650^oC	28

LIST OF FIGURES

S.no	Title	Page no
3.1	Phase Diagram of Y_2O_3-Al_2O_3 System	12
3.2	Flow Diagram for the Processing of the Al_2O_3-YAG composites	13
3.3	Schematic diagram of Vickers hardness indenter	15
3.4	Schematic diagram of 3-point flexure strength test	16
4.1	DSC/TG, Alumina – 40 mol% Y_2O_3 (as Yttrium Nitrate)	19
4.2	DSC/TG, Alumina – 50 mol% Y_2O_3 (as Yttrium Nitrate).	20
4.3	DSC/TG, Alumina – 60 mol% Y_2O_3 (as Yttrium Nitrate).	20
4.4	XRD pattern of Alumina- 40 Mole % of Y_2O_3 calcined at different temperature	21
4.5	XRD pattern of Alumina- 50 Mole % of Y_2O_3 calcined at different temperature	21
4.6	XRD pattern of Alumina- 60 Mole % of Y_2O_3 calcined at different temperature	22
4.7	XRD pattern of Alumina40 Mole % of Yttrium Aluminate Of Composites	23
4.8	XRD pattern of Alumina50 Mole % of Yttrium Aluminate of Composites	24

4.9	XRD pattern of Alumina60 Mole % of Yttrium Aluminate of Composites	24
4.10	Relative density of sintered sample at 1650^{o}C	26
4.11	Apparent Porosity of sintered sample at 1650^{o}C	26
4.12	Hardness of sintered sample at 1650^{o}C	26
4.13	flexural strength of sintered sample at 1650^{o}C	28
4.14	Microstructure of Sintered Alumina-60 Mole % of Yttrium Aluminate 20 vol % Composites	29
4.15	Crack path in the indented samples (a) Pure Alumina (b) Alumina- 20 vol% YA (40 mol%)	30
4.16	Crack path in the indented samples (a)Alumina- 20 vol% YA (50 mol%) (b) Alumina- 20 vol% YA (40 mol%)	30

Chapter-1

INTRODUCTION

Alumina is one among the important ceramic materials both for traditional as well as for advanced applications. Among its diversified application areas, some of the key areas are grinding tubes, crucibles and tubes for high-temperature applications, cutting tool inserts, etc. The properties of Alumina that result in this application are high corrosion and erosion resistance, impact resistance, high-temperature stability. However, low fracture toughness and brittle fracture behaviour of Alumina puts a limitation on the widespread application of alumina. Many methods have been tried to improve the resistance to crack propagation or, in other words, fracture toughness. Ductile metals such as (Cu, Ni) have been added to Alumina in order to impart ductility and higher toughness. This method has resulted in the development of Cu-Alumina and Ni-Alumina composites [1]. The use of TiC in Alumina have not only the toughness and strength but it has also improved the overall thermal conductivity and hence the thermal shock resistance [2]. On the other hand, the combination of Alumina and different Stabilized Zirconia (Y-TZP, Y-PSZ) have also been successful in creating a tough ceramics (ATZ and ZTA). All the ideas discussed above dealt with two distinct phase which are the virtually non-interacting type. The toughness improvement in these above cases result from dispersion strengthening and transformation toughening, respectively. But there are certain other additives like SrO and Y_2O_3 which when added to Alumina produce the corresponding Aluminate phase (Strontium Aluminate or Yttrium Aluminate respectively) which can also improve the crack propagation resistance [3]. However, the improvement, in this case, can be attributed to the elongated particle morphology that provided the crack bridging effect. Cutler et al had observed that the addition of 15 vol % SrO to Ce-TZP/Al_2O_3 yielded elongated $SrZO_3$ into in the matrix that improved the strength and toughness [4]. Lach et al [5] reported that Y_2O_3 addition in Al_2O_3 results in YAG phase formation that improved the toughness. The toughness increment was due to the higher crack growth resistance of YAG phase. It was also reported by Rana [6] while working on Al_2O_3-YTZP composite that even a small fraction of

YAG could improve the mechanical properties of Al_2O_3-YTZP. In view of these observations, it was thought that addition of Y_2O_3 to Alumina for deliberate generation of YAG in situ in Alumin is also expected to affect the densification and the fracture behaviour of the composites. In view of the above facts, it was thought worthwhile to study the following aspects:

(a) Study of the effect of different Al_2O_3-Y_2O_3 molar ratio on the different Yttrium Aluminate compositions. Normally, YAG is the most desired phase in the Al_2O_3-Y_2O_3 system. However, depending on the molar ratio of Al_2O_3-Y_2O_3, YAM and YAP (the two other phases of Al_2O_3-Y_2O_3) may also form. Therefore, it will be interesting to study the effect of YAM and YAP phases on the densification, strength and toughness of the composites.

(b) The incorporation of processed Yttrium Aluminate in different volume fraction to Alumina and to study the densification behaviour

(c) The study of strength toughness and microstructure of the Alumina-YAG/YAM/YAP composites

Chapter-2

LITERATURE REVIEW

Medraj et al. [7] studied the phase formation in the Al_2O_3–Y_2O_3 system by prepared through solid state mixing route. XRD study showed that the stoichiometric YAG composition (mol% Al_2O_3: Y_2O_3 :: 62.5 :37.5) phase start appearing from 1200ºC. With the increase in temperature from 1200ºC to 1600ºC, higher amount of YAG phase was observed at the expense of Al_2O_3-Y_2O_3. However, even at 1600ºC, YAG formation was incomplete and unreacted Y_2O_3 and Al_2O_3 could be detected. In view of the above finding, it was concluded that in the solid state mixing route using Al_2O_3–Y_2O_3 1900ºC or higher temperature is required for the complete conversion of entire Y_2O_3 to YAG.

Lima et al. [8] studied the solid state powder processing route for YAG preparation. A stoichiometric Al_2O_3–Y_2O_3 powder mix was milled and calcined at different temperatures viz. 1000°C, 1200°C, 1400°C & 1600°C for 3 hours. It was observed that the complete equilibrium conversion to YAG was possible at 1400ºC through the intermediate phase of $YAlO_3$.

Nagira et al. [9] studied the fabrication Al_2O_3-YAG eutectic composition prepared by undercooled melt solidification process. The eutectic composition was prepared the polymeric complex method. The microstructure of equilibrium eutectic composition differed from that of the metastable eutectic composition. The fracture strength increased with YAG addition to Al_2O_3.

Lach et al. [10] studied the synthesis of Al_2O_3-YAG 20 vol % composite by co-precipitation method using Aluminium Nitrate and Yttrium Nitrate as the precursor and Ammonium Carbonate as the precipitating agent. The as precipitated powder contained an amorphous Ammonium Aluminium Carbonate in which Y_2O_3 was embedded. At 800ºC, γ-Al_2O_3 appeared followed by the crystallization of δ-Al_2O_3 and θ-Al_2O_3 at 1100ºC. At 1198°C, α-Al_2O_3 and YAG also appeared. The presence of YAG limited the grain growth of the Al_2O_3 matrix.

Lach et al. [5] studied the processing of Alumina - YAG composites in which the YAG content was varied between 5-30 vol%. It was observed that YAG addition retarded the densification

of Alumina. Fracture toughness was calculated by indentation method, and a high fraction of YAG decreased the toughness as well as strength. It was also observed that there was a marked difference in the crack path of Alumina & YAG composite. While the former exhibited a rather a straight crack path, Al_2O_3 – YAG composite showed a zigzag path. It was concluded that the presence of YAG phase slowed down the crack propagation by increasing the crack propagation path length. This difference in the crack path length was responsible for the enhancement of strength and toughness value of the composites.

Voytovych et al. [11] studied the effect of Y_2O_3 addition on the densification and coarsening behaviour of Al_2O_3-Y_2O_3.The addition was accomplished through the mixing of $Y(NO)_3.6H_2O$ and Al_2O_3 in different proportions (0-3000 wt % ppm Y_2O_3) They observed that Y_2O_3 – doping inhibited the densification of Al_2O_3 till 1450^{o}C, the effect was least at 1550^{o}C and no effect could be observed for the samples sintered at 1650^{o}C.

Sommer et al. [12] studied the effect YAG preparation route on the properties of Al_2O_3-YAG composites. The percentage of YAG was varied as 5, 10 and 20 vol % in the composite matrix. The addition of YAG was carried via two different processing routes. In one of the routes, previously prepared YAG powder was mixed with alumina. In the other process, prerequisite amount of Y_2O_3 (as $Y(NO_3)_2$) was coated during the powder processing step to form YAG on calcination. Three different compositions (5, 10 and 20 vol %) of slurries were prepared by slip casting method. It was observed that irrespective of the YAG processing method, the Relative density of Al_2O_3-10 vol % YAG composite showed the best properties. It was concluded that the presence of YAM and YAM in the coated powder resulted in an improvement in properties. Hardness, Flexural Strength and Fracture Toughness was maximum at 10 vol% addition. As the YAG percentage increases to 20 vol%, it was difficult to sinter due to the inhomogeneous distribution of YAG phase in the composite.

Palmero et al. [13] compared the various sintering routes for the preparation of Al_2O_3-YAG nanocomposites. The composites were prepared by wet-chemical synthesis route using Al_2O_3-YAG by 50 vol %. Alumina-YAG composite powder was synthesized at 25^oC using inverse co-precipitation by the reverse strike method. In some sample 500 ppm, MgO was also added. When the sample was calcined at 900^oC, the grain size was 20 nm. The grain size reached 120 nm at 1200^oC. MgO – doped sample showed very less effect on the grain growth. When the compacts were fabricated and sintered at low sintering temperature 1420^oC, a fine microstructure was found where Al_2O_3 and YAG grains were less than 200 nm in size.

Pastor et al. [14] studied the processing and mechanical properties of unidirectionally solidified Alumina–YAG composite both at Room Temperature as well as at High Temperature. Laser floating zone method was used to grow the rods of diameter 1 mm. The longitudinal strength showed a linear rise in growth rate. The transverse strength reduced from 144to 118MPa as the growth rate rises from 25 to 750 mm/hr. The low transverse strength of the rods was due to the presence of elongated flaws focused along the axis of growth. Hardness increased somewhat with the development rate while the toughness didn't show any huge difference. The hardness was undistinguishable in the longitudinal & transverse directions. The longitudinal strength of the rods was determined from the flexural test. The strength was constant till 1427^oC and reduced at 1627^oC. The homogeneous microstructure was eroded at 1627$^oC$was observed which was also associated with the decrease in the longitudinal strength.

Palmero al. [15] studied the preparation of Alumina–YAG micro-composite through doping of $YCl_3 \cdot 6H_2O$ in order to obtain 5 vol% YAG in the composite powder. The effect of YAG on the mechanical properties of Alumina was investigated. The samples were prepared by Pressureless Sintering at 1500^oC for 3h, Hot Pressing at 1450^oC for one hr and Spark plasma sintering at 1350^oC and 1450^oC at 75 MPa. High hardness and toughness was observed in the Hot Pressed samples as compared to that obtained from pressureless sintering. Even the spark

plasma sintering materials showed high hardness value. The fine doping of YAG in Alumina helped to reach the theoretical density

Duong et al. [16] studied the creep behaviour of two fine-grained 1600^{o}C sintered Alumina–YAG (50 vol % Al_2O_3 -YAG and 25 Vol % Al_2O_3 – 75 vol % YAG) composite material. The creep properties were tested in the temperature range of 1400^{o}C -1500^{o}C at a stress level of 3 to 20 MPa. No dynamic grain growth resulted during creep and the stress exponent values were nearly the same, 1.1 + 0.1 and independent of the temperature. The activation energies of creep was 612 KJ mol^{-1} for the 50% YAG material composite and 592 KJ mol^{-1} for the 75% Yttrium Aluminate Garnet material (YAG) composite.

Ochiai et al. [17] studied the deformation & fracture behaviour of Alumina and YAG composites from 25^{o}C to 1750^{o}C. The samples were prepared by Unidirectional Solidification process. The deformation behaviour was found to depend on the displacement rate. At a displcement speed of 8.3×10^{-6} m/s, the samples were found to be brittle in nature. However, when the displacement rate and temperature increased to 8.3×10^{-7} m/s ductile fracture behaviour was observed.The crack was found to propagate mainly through YAG grains having lower ductility. The fractured area of Yttrium Alumina Garnet (YAG) in the fractured surface was found to be higher.

Waku et al. [18] studied high temperature strength and thermal stability of the unidirectional solidified Al_2O_3 –YAG eutectic composites. SEM microstructure showed single crystal Al_2O_3 and single crystal YAG. The plastic deformation was 10-20 %, and yield stress is around 200 MPa at 1650^{o}C. SEM confirmed the thermal stability of the microstructure. When the sample was heat-treated at 500,700 & 1000 hr of heat treatment at 1650^{o}C no grain growth could be observed. It was proposed that the excellent high temperature strength characteristics was due to the single crystal eutectic structure, absence of an interface and the presence of YAG.

Rico et al. [19] studied the plastic behaviour of directionally solidified Alumina–YAG eutectics. The microstructure exhibited similar morphologies for both the Al_2O_3 and YAG phase. It was concluded that both bulk diffusion and dislocations contributed to the creep. When the stress or interphase spacing was increased, then the role of dislocation became important.

Chapter-3

EXPERIMENTAL WORK

Raw Materials

The raw materials for this study were Alumina(Al_2O_3) (Almatis India), Yttrium Oxide (Y_2O_3) (LobaChemie, India).

3.1 Powder Processing

The processing step for Al_2O_3-Yttrium Aluminate composite consists of the following steps:

1. Synthesis of Yttrium Nitrate [$Y(NO_3)_2$] solution
2. Preparation of Al_2O_3-Yttrium Nitrate powder mix.
3. Calcination of powder mix (as in 2.), for Yttrium Aluminate phase transformation.
4. The addition of different volume fraction of Yttrium Aluminate in Alumina matrix to prepare Al_2O_3-yttrium Aluminate composite powder.
5. Compaction & sintering of the composite.
6. Characterization

3.1.1 Synthesis of Yttrium Nitrate

Yttrium nitrate solution was synthesized by dissolving Y_2O_3 in 1:3 HNO_3. 100 grams $Y_2O_3$is slowly added to 500 ml acid solution 1:3 HNO_3 solution while the acid solution was being stirred to dissolve in HNO_3 at 70^oC. Stirring was continued for 4 hours for ensuring completed dissolution of Y_2O_3 in HNO_3. The obtained solution was cooled to room temperature and filtered through Whatman Filter (542) paper and stored in a sealed glass bottle.

3.1.2 Estimation of Yttrium Nitrate Solution

1 ml of yttrium nitrate was taken in a pre-weighted platinum crucible. NH_4OH was added dropwise in excess to precipitate $Y(OH)_3$. The platinum crucible was dried in an oven. The dried precipitate was fired at 1000^oC and weighed The difference in weight provided the weight of Y_2O_3 per ml of the $Y(NO_3)_2$ solution.

3.1.3 Preparation of Al_2O_3 –$Y(NO_3)_2$ powder mix and Calcination

For the preparation of Al_2O_3-$Y(NO_3)_2$ mix, Yttrium Nitrate solution (in different mol %) was mixed with calcined alumina. Following the Al_2O_3 –Y_2O_3 phase diagram (Fig-3.1), the mol % of Y_2O_3were 40, 50 and 60 %. Required volume of Yttrium Nitrate was added to Al_2O_3 powder and was thoroughly mixed in agate mortar & pestle for 1 hours. The sticky mass was dried at 60^{o}C in an oven, and the dried mass was calcined at three different calcination temperatures viz. 1200^{o}C, 1300^{o}C and 1400^{o}C.

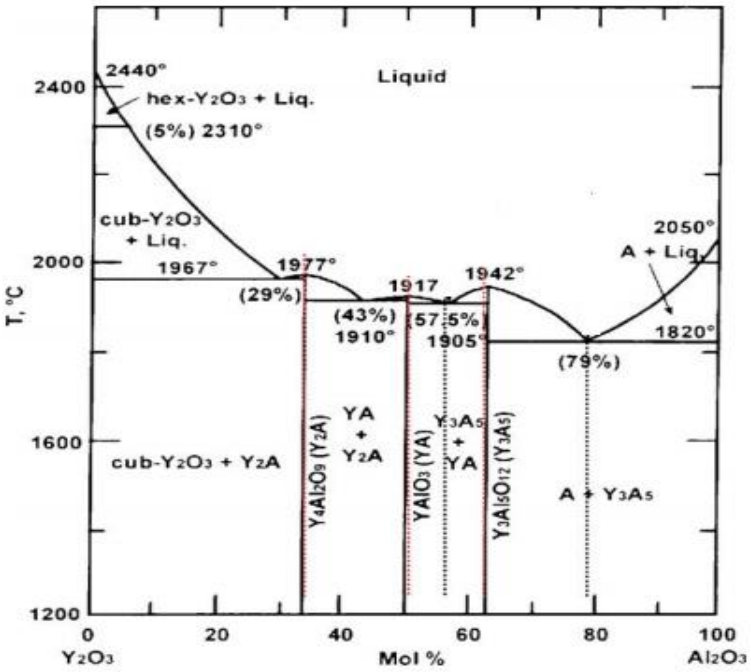

Fig-3.1 Phase Diagram of Y_2O_3-Al_2O_3 System [7].

3.1.4 Compaction and Sintering

Although Al_2O_3-$Y(NO_3)_2$powder mix was calcined at three different temperatures, a study of XRD patterns of the 1400^{o}C calcined powder yielded the desired phase. Therefore, only the 1400^{o}C calcined powders were user for further processing of Al_2O_3- Yttrium Aluminate Garnet (YAG) composites.

3.1.5 Processing of Al_2O_3-YAG Composites

Varying volume fraction (5, 10, 15 & 20 %) of calcined yttrium Aluminate phase was mixed with Al_2O_3powder. The two powders were first dry mixed in an agate mortar followed by wet milling in propanol medium for 8 hours. The milled power was dried and mixed with 5 % PVA and compacted into a rectangular bar (60 x 5 x 5 mm). The compacted sample were sintered at 1650^{o}C for 2 hours. The sintered sample were characterizedfor apparent porosity, bulk density, hardness, bending strength, fracture toughness and microstructure.

3.2 **Flowsheet for Processing of theAl_2O_3-YAG Composites.**

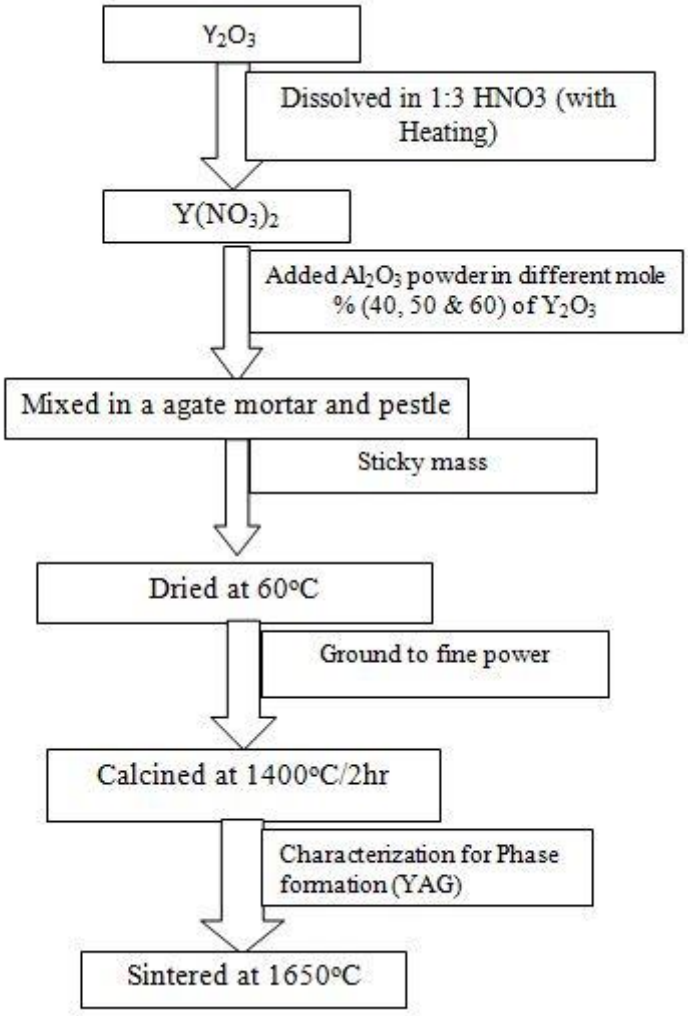

Fig-3.2 Flow Diagram for the Processing of the Al_2O_3-YAG Composites.

3.3Characterization

3.3.1 Thermal decomposition behaviour of Al_2O_3 Yttrium Nitrate powder mix

Differential Scanning Calorimetry and Thermogravimetry is done by NETZSCH STA 449 C, in a Netzsch simultaneous in an argon atmosphere at a heating rate of 10^{o}C/min DSC/TG instrument (STA 449) upto 1500^{o}C.

3.3.2 XRD

The phase analysis of the calcined powder and sintered samples of alumina-Yttrium Aluminate were carried out by an X-ray Powder Diffractometer (Rigaku,Miniflex II, Japan). Calcined samples and sintered samples at different temperature was broken into small pieces and ground into fine powder. X-ray generator was operated at 35kV voltage and 15 mA current. Cu Kα radiation with λ = 1.54Å was used as the incident radiation. The samples were scanned in the 2Θ range 20-80^o at a scan speed 0.02^o per second. The analysis of obtained diffraction pattern was done by matching them with standard XRD patterns by using Philips X-Pert High Score software.

3.3.3 Bulk Density and Apparent Porosity

The bulk density and apparent porosity of the sintered pellets were measured by Archimedes principle using water as the immersion liquid. As per ASTM standard C-20, the dry weight of the specimen was measured followed by filling the open pore of thespecimen in water. The water was boiled for an hour to confirm filling of the entire pore. Similarly, the suspended weight of the specimen was also measured while keeping the specimen suspended in the liquid. The bulk density and the apparent porosity were calculated using the suspended and soaked weight.

$$\text{Bulk Density} = \left(\frac{W_d \times density\ of\ liquid}{W_{SK} - W_{SU}}\right) \times 100 \qquad (3.1)$$

$$\text{Apparent Porosity} = \left(\frac{W_{sk} - W_d}{W_{SK} - W_{SU}}\right) \times 100 \qquad (3.2)$$

3.3.4Vickers Hardness

The Vickers hardness of the sintered Al_2O_3-Yttrium Aluminate Garnet (YAG) samples tested in a Semi Macro Hardness Tester (Leco, LV700). The faces of the rectangular bar were ground with 800 grade & 400 grade SiC powder to obtain a parallel and smooth surface. The edges of the bars were also chamfered with SiC. The polished samples were indented at three different loads, 3, 5 & 10 Kgf for 10 seconds. Higher loadswere avoided because they resulted in extensive cracking from the diagonal corner. A plot was made between half diagonal lengths of the indent against indentation load [19]. The hardness was calculated from theslope of the plot using the following relation. (3.3)

$$H_v = 0.47 \times \left(\frac{P}{a^2}\right) \tag{3.3}$$

Where, H_V is the Vickers hardness (GPa), P is applied load (N) and ais the half diagonal length (μm).

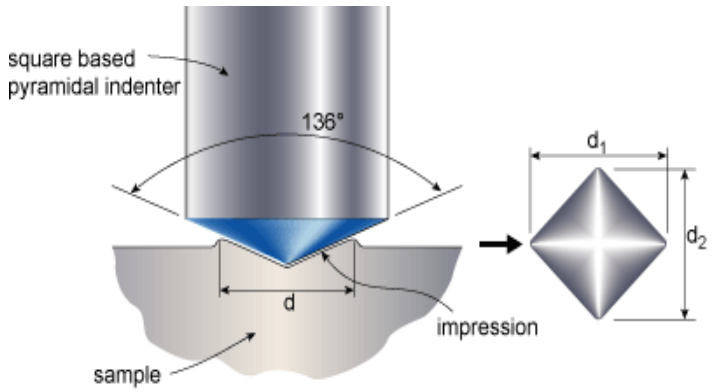

Fig3.3:-Schematic diagram of Vickers hardness indenter.

3.3.5 Flexural Strength

The three-point bending strength of the sintered samples or the flexural strength were measured by the Universal Testing Machine (HK10S, Tinus Olsen, U.K) with a span length of 40 mm and crosshead speed 0.1 mm/sec [20].The edges of the rectangular bars were ground and chamfered with 800 grade & 400 grade SiC powder to obtain a parallel and smooth surface. The three-pointstrength was calculated from the equation (3.4)

$$\sigma_f = \frac{3PL}{2bd^2} \quad (3.4)$$

Where, P = Fracture load, L = Span length, b = Width of the sample, d = Depth or thickness of the sample.

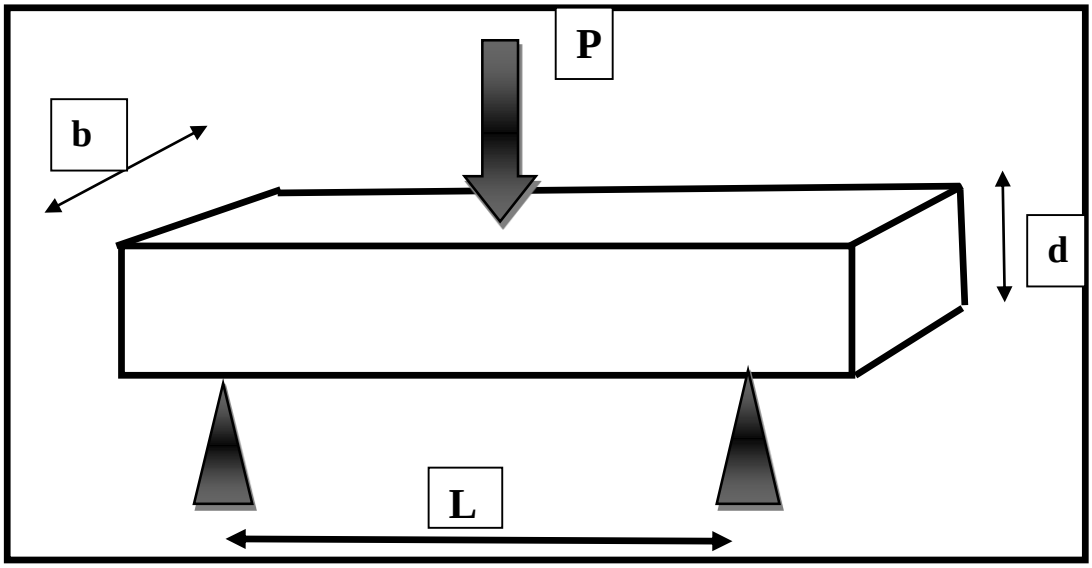

Fig3.4:-Schematic diagram of 3-point flexure strength test.

3.3.6 Fracture Toughness

The fracture toughness of the sintered specimen were measured by Indentation Strength in Bending (ISB) method [21]. The edges of the rectangular bar were ground with SiC powder to obtain a parallel and smooth surface. In this method, an indent was made by Vickers Indenter at the centre of the tensile surface of the specimen. The indentation load was 20 Kgf. Radial cracks originated from the diagonal of the indent that served as the pre-crack for the test. The indented specimens were broken in the three-point bending method at a crosshead speed is 0.5 mm/sec.The fracture toughness $K_{ic}$was calculated from the following equation (3.5).

$$K_{ic} = \eta\,(E/H)^{1/8}\,(\sigma_f P^{1/3})^{3/4} \quad (3.5)$$

Where η is the geometrical constant (0.59),H the Vickers' hardness, E the Elastic Modulus and P is the Indentation load.

3.3.7 Microstructure of Sintered Specimens

The microstructure of sample was observed by FESEM (Nova Nanosem 450 FEI). The samples were coated with Platinum for 7 min to make the surface conducting. The fractured and indented samples were also observed in Backscattered electron (BSE) mode at an accelerating voltage of 10KV.

Chapter-4

RESULTS AND DISCUSSION

4.1 Decomposition behaviour of Yttrium Nitrate and Crystallization of Yttrium Aluminate

Fig- 4.1, 4.2 & 4.3 shows the DSC/TG plot of Alumina - Yttrium Nitrate powder mixture having 40, 50 and 60 mol % Y_2O_3 respectively. All the three curves show a series of endothermic peaks between 70^{o}C to 600^{o}C. These peaks correspond to the melting of Nitrates, Dehydroxylation of Yttrium Nitrate to oxy-nitrate. All these processes are over 600^{o}C. Around 600^{o}C, a broad exothermic peak is observed which is likely to account for the formation of Y_2O_3. Between 900^{o}C -1200^{o}C, a broad exothermic peak is again observed along with a distinct exothermic peak around 1200^{o}C. A gradual weight gain is observed between 1100-1200^{o}C. These two features indicate that the exothermic peak at 1150^{o}C correspond to Yttrium Aluminate formation [22].

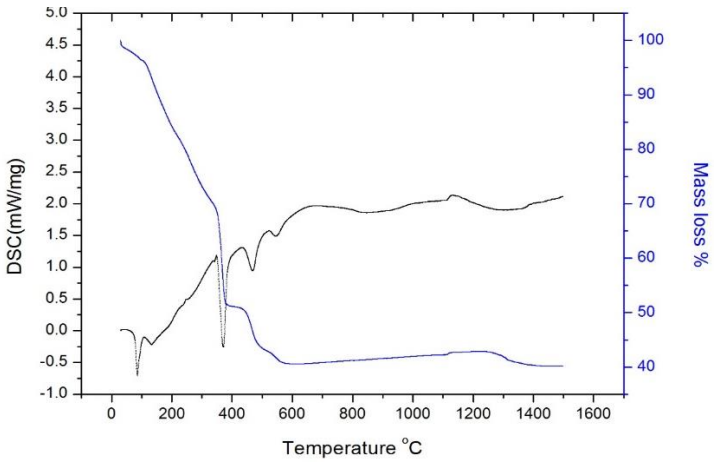

Fig 4.1:-DSC/TG, Alumina – 40 mol% Y_2O_3 (as Yttrium Nitrate).

It can be further observed from the DSC plots that the broad exothermic peak between 600 - 800^{o}C increases in intensity at higher Y_2O_3 content. On the other hand, the small and broad exothermic peak at 1200^{o}C (40 mol% Y_2O_3) shifts slightly to a lower temperature at 50 mol% Y_2O_3 composition. At 60 mol% Y_2O_3, the 1150^{o}C peak disappears and the exothermic peak at 800^{o}C becomes the dominating peak. A correlation with the XRD patterns of all the three compositions leads to the following conclusions:

The exothermic peak at 1200^{o}C correspond to the YAG phase formation. The peak between 800^{o}C -1200^{o}C corresponds to YAP formation. AS the YAP peaks becomes stronger and the YAG peaks become weaker at higher Y_2O_3, the DSC peak at 800^{o}C becomes the dominating peak the one at 1200oC becomes the weak peak. Thus the nature of the DSC curve changes with the composition.

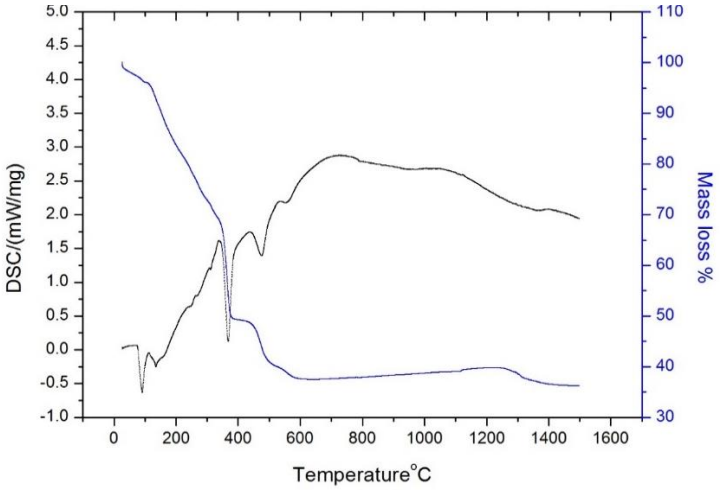

Fig 4.2:- DSC/TG, Alumina – 50 mol% Y_2O_3 (as Yttrium Nitrate).

.

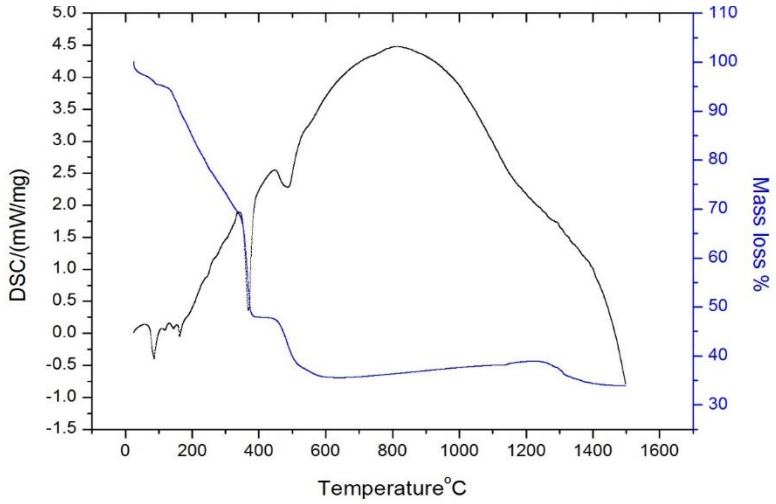

Fig 4.3:- DSC/TG, Alumina – 60 mol% Y_2O_3 (as Yttrium Nitrate).

4.2 Phase evolution in the calcined Al_2O_3-Y_2O_3 powder

All the Al_2O_3 –Y_2O_3 composition were calcined at three different temperatures 1200^{o}C, 1300^{o}C & 1400^{o}C.

4.2.1 Phase Evolution in Al_2O_3-40 mol % Y_2O_3

In this composition, at 1200^{o}C, no Yttrium Aluminate Garnet (YAG) phase forms. Fig-4.4 shows that with the increase in calcinations temperature from 1200°C to 1400°C, Yttrium Aluminate Garnet (YAG) phase appears and its fraction is the highest at 1400°C. The other two phases Yttrium Aluminate Monoclinic (YAM) and Yttrium Aluminate Perovskite (YAP)

(transient Yttrium Aluminate phases) which forms at 1200°C decreases at 1400°C through Yttrium Aluminate Perovskite (YAP) is present 1400°C.Although, at 1200°C, $Y_2O_3$and Al_2O_3 could be observed at1400°C, no free Al_2O_3 could be detected.

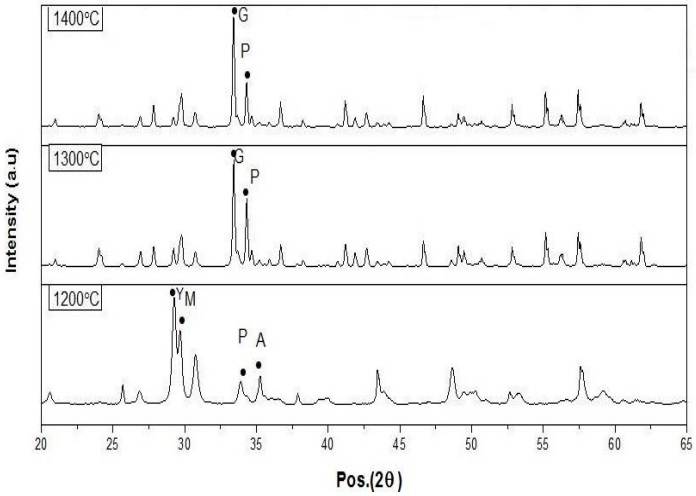

Fig-4.4:- XRD pattern of Alumina- 40 Mole % of Y_2O_3 calcined at different temperature:

4.2.2 Phase Evolution in Al_2O_3-50 mol % Y_2O_3

Fig-4.5 shows the XRD of Al2O3- 50 mole %Y_2O_3 samples calcined at 1200ºC, 1300ºC & 1400ºC. In this composition at 1200ºC, only Yttrium Aluminate Perovskite forms which react with Y_2O_3 to form the Yttrium Aluminate Garnet at 1300ºC. At 1400ºC, the composition contains all the three phases of Yttrium Aluminate viz.Yttrium Aluminate Monoclinic, Yttrium Aluminate Perovskiteand Yttrium Aluminate Garnet along with free Y_2O_3.

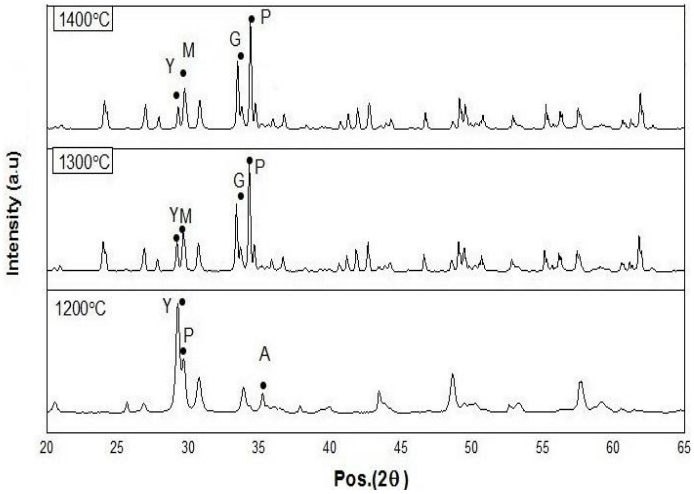

Fig-4.5:-XRD pattern of Alumina-50 Mole % of Y_2O_3 calcined at different temperature.

4.2.3 Phase Evolution in Al_2O_3-60 mol % Y_2O_3

In the Al_2O_3 60 mole % Y_2O_3, composition the YAG phase is the lowest, and the two higher fractions phase are Yttrium Aluminate Monoclinic and Yttrium Aluminate Perovskite. These only at 40 mole % Y_2O_3, maximum Yttrium Aluminate Garnet (YAG) forms. At 50 and 60 mole % all three phases' viz. YAG, YAP & YAM phases are present. The trend follows the established Al_2O_3-Y_2O_3 phase diagram (Fig-3.1).

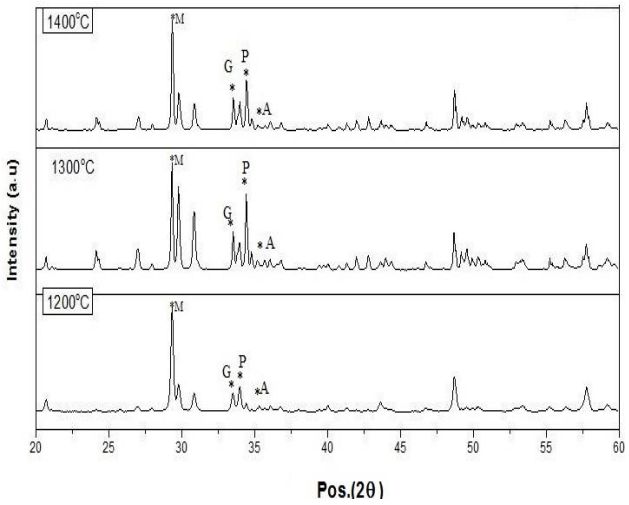

Fig-4.6 XRD pattern of Alumina- 60 mole % Y_2O_3 calcined at different temperature.

4.3 Phase analysis of sintered Al_2O_3- Yttrium Aluminate of composites

For preparing the composites, different volume percentage (5, 10, 15 & 20 vol %) of calcined Yttrium Aluminate was added to alumina. Corresponding to each Yttrium Aluminate composition (ie. 40 mole %, 50 mole % and 60 mole %), four different composites were prepared with 5, 10, 15 & 20 vol % of Yttrium Aluminate being introduced in Aluminamatrix. The power mix was compacted into rectangular bars (60 mm x 5 mm x 5 mm) and sintered at 1650^{o}C for 2 hours. XRD patterns of the sintered sample contained only Al_2O_3 and YAG phase. Neither any free Y_2O_3 nor any of the intermediate phases of Yttrium Aluminate (viz. YAM & YAP) could be detected. The results further show that the relative value of YAG /Al_2O_3 increases with increase the in the vol % of Yttrium Aluminate phases in Al_2O_3. The results could be explained as follows:

In the calcined sample, besides YAG, YAP & YAM phases appear as the composition deviated from the stoichiometric YAG composition (37 mol % Y_2O_3). This resulted in YAM and YAP phases in the calcined samples. However, when such calcined samples were added to Al_2O_3 and sintered at 1650^oC, more Alumina was able to react with Yttrium Aluminate and form YAG phase. Since the volume fraction of Yttrium Aluminate was rather small (upto 20 vol %), it produced YAG as the only Yttrium Aluminate phases in the sintered sample, but the fraction of YAG also increased with the increase in Yttrium Aluminate phase because even at the highest vol % (20 vol %) the composition was predominately Al_2O_3 rich. Therefore, such a composition during sintering could readjust the Al_2O_3:Y_2O_3 molar ratio to YAG composition and, therefore, only YAG and Al_2O_3 phases were present in the sintered composites. Following the same logic, 20 vol % Yttrium Aluminate resulted in a higher fraction of YAG as a compound to 5 vol % Yttrium Aluminate addition.

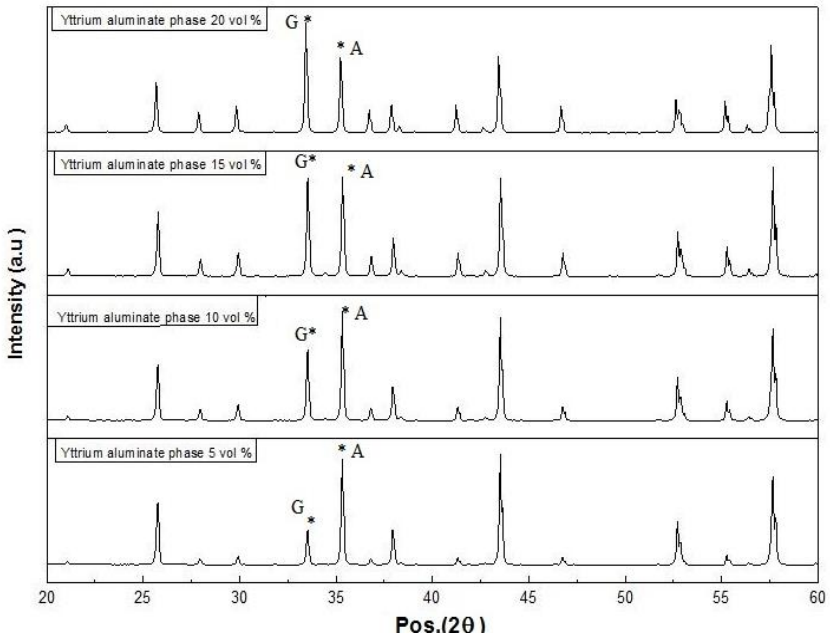

Fig-4.7:-XRD pattern of Alumina-40 Mole % of Yttrium Aluminate of Composites.

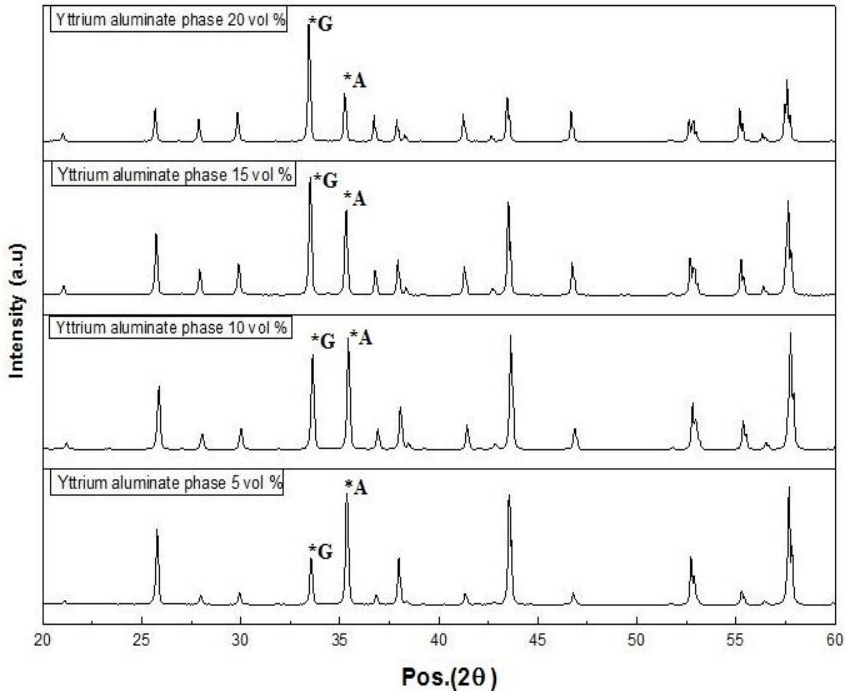

Fig-4.8:-XRD pattern of Alumina-50 Mole % of Yttrium Aluminate of Composites.

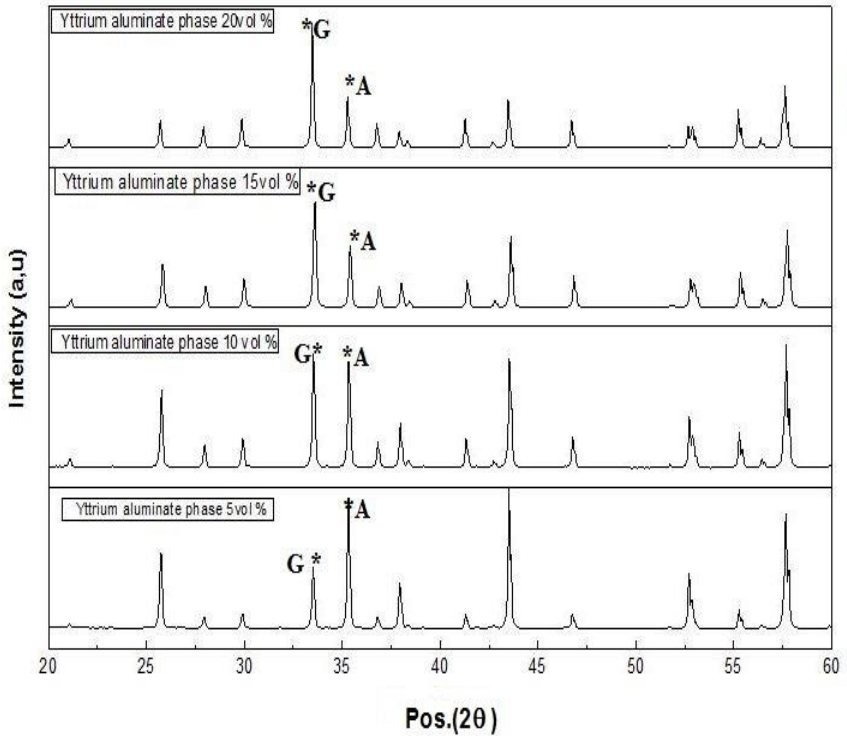

Fig-4.9:- XRD pattern of Alumina-60 Mole % of Yttrium Aluminate of Composites.

Table 4.1: Relative Fraction of Al_2O_3 and YAG in the Sintered Samples of Alumina-Yttrium Aluminate of Composites

Vol% Yttrium Aluminate in Al_2O_3	Molar Composition of $YAlO_3$					
	Al_2O_3: Y_2O_3::60:40		Al_2O_3: Y_2O_3::50:50		Al_2O_3: Y_2O_3::40:60	
	Vol% Al_2O_3	Vol% YAG	Vol% Al_2O_3	Vol% YAG	Vol% Al_2O_3	Vol% YAG
5	74	26	70	30	67	33
10	59	41	53	47	48	52
15	48	52	41	59	36	64
20	42	58	31	68	24	76

4.4 Bulk Density and Relative Density of Sintered Alumina as a function of Yttrium Aluminate of Composies.

Table-4.1shows that the addition of Yttrium Aluminate to Alumina initially increases the relative density till 15 vol % Yttrium Aluminate addition. At 15 vol % additives, the relative density is the highest (94 %) at 60 mol% Y_2O_3 composition. The density decreases at higher volume percent (20 vol %) Yttrium Aluminate addition. In general, it may be said that the in-homogeneous distribution of Yttrium Aluminate Garnet (YAG) in Al_2O_3 matrix probably retarded densification. The other important factor which can contribute to poor density is the volume expansion associated with YAG formation. A molar volume expansion of 2% takes place as a result of YAG formation. This volume expansion could also have contributed to the poor densification. Similar trend in the densification behaviour has been observed for Al_2O_3-ZrO_2 composites where, the maximum densification is usually observed between 10-15 vol % ZrO_2 additives.

Table-4.2:-Relative density of Yttrium Aluminate phases in alumina.

Vol % Yttrium Aluminate in Alumina	Relative Density of Sintered Al_2O_3	Relative Density of Sintered Alumina-Yttrium Aluminate (YA) Composites with different Al_2O_3: Y_2O_3 molar ratio in Yttrium Aluminate		
		40 mole %	50mole %	60mole %
0	90	-	-	-
5	-	81.70	82.87	85.24
10	-	82.70	82.47	87.16
15	-	88.3	90.84	94.02
20	-	83.82	82.4	84.50

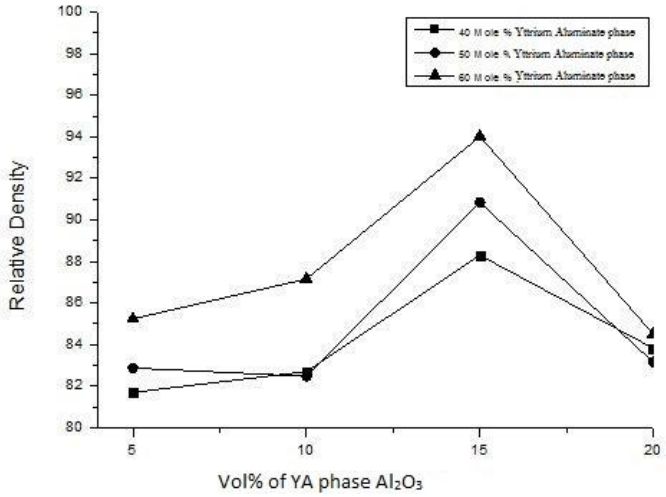

Fig-4.10:-Relative density of sintered sample at 1650^{o}C.

4.5 Apparent Porosity of Sintered Alumina as a function of Yttrium Aluminate of composites.

The apparent porosity follows the inverse trend of relative density, and minimum apparent porosity was obtained at 15 vol % Yttrium Aluminate addition to Al_2O_3 (Fig-4.11).

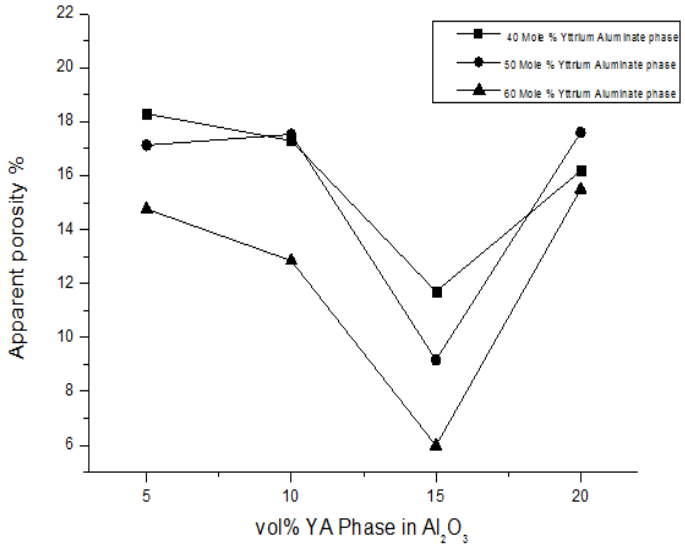

Fig-4.11:-Apparent Porosity of sintered sample at 1650^{o}C.

4.6 Hardness of Sintered Alumina as a function of Yttrium Aluminate of composites.

The Vickers Hardness of the Alumina-Yttrium Aluminate Composites is shown in Fig 4.12. The hardness follows the same trend as that of density and the maximum hardness of 10 GPa was obtained for 60 mol% composition at 15 vol% Yttrium Aluminate addition. The hardness decreased at higher volume percent of Yttrium Aluminate probably due to agglomeration effect and non-uniform densification.

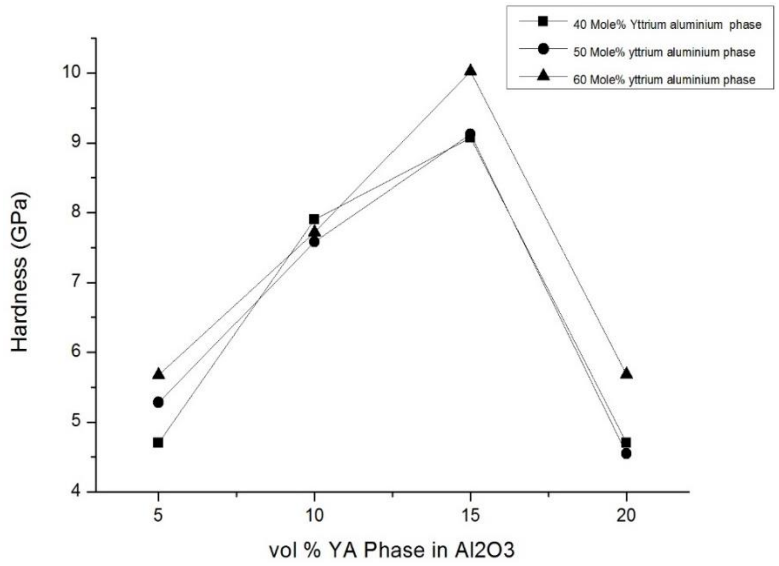

Fig-4.12:-Hardness of sintered sample at 1650^{o}C.

4.7 Flexural Strength of Sintered Alumina as a function of Yttrium Aluminate of composites.

The flexural strength of the Alumina-Yttrium Aluminate Composites is shown in Fig-4.13, and for the pure Alumina sample the fracture strength was 86.6 MPa. The flexural strength follows the same trend of that of density and maximum flexural strength of 154 MPa was obtained for 60 mol% composite at 15 vol% Yttrium Aluminate addition. The flexural strength decreased at higher volume percent of Yttrium Aluminate probably due to agglomeration effect and non-uniform densification.

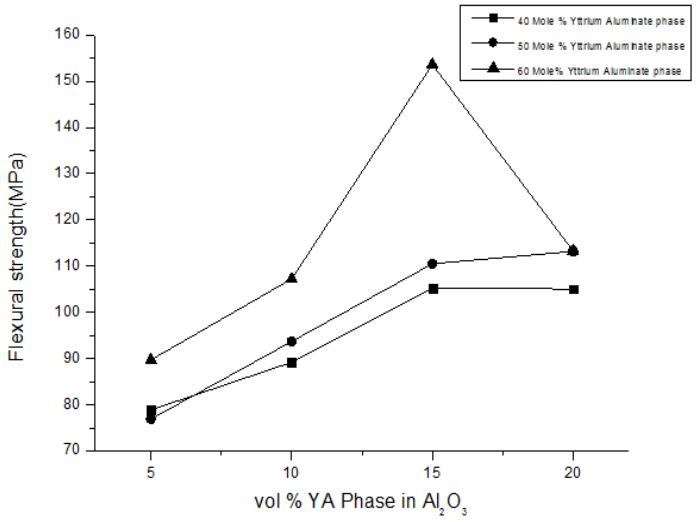

Fig-4.13:-Flexural strength of sintered sample at 1650^{o}C.

4.8 Fracture Toughness of Sintered Alumina as a function of Yttrium Aluminate.

The fracture toughness could be measured only for 15 and 20 vol % Yttrium Aluminate added sample. For other composites, high porosity in the sintered made it difficult to identify the indent and hence the hardness. The toughness was highest at 15 vol % addition (4.1 MPa $m^{1/2}$) for 60 mol% Y_2O_3 composition and it was significantly higher than that of pure Alumina (2.2 MPa $m^{1/2}$). The increase in toughness was due to the increase in crack path deviation or crack bowing. Similar results have also been reported by Sommers at al [12] and Lach et al [5]. It was also observed (Table 4.1), that the compositions which exhibited high toughness also had YAG to Al_2O_3 volume fraction ratio of nearly 2. Thus, the presence of both YAG and Al_2O_3 phase is important for achieving a higher strength and toughness

Table 4.3:- Fracture toughness of sintered sample at 1650^{o}C.

Vol % Yttrium Aluminate in alumina	Fracture Toughness (MPa√m) of Alumina-Yttrium Aluminate (YA) Composites with Y_2O_3 different content in YA		
	40 mole %	50 mole %	60 mole %
15	3.4	3.56	4.1
20	2.71	2.72	2.9

4.9 Microstructure of Sintered Specimen Alumina-YAG Composites.

The microstructures of the sintered samples show YAG phases as bright phase and Al_2O_3 as dark phase (in BSE mode). The sintered sample is porous, and the distribution of YAG is not uniform. At many places, a cluster of YAG could be seen (Fig.4.14, encircled area). This probably caused poor densification. Similar microstructure could be observed for all the compositions.

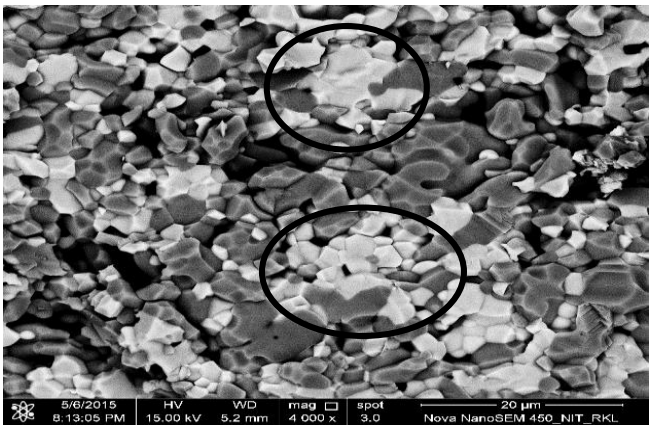

Fig- 4.14:- Microstructure of Sintered Alumina-60 Mole % of Yttrium Aluminate 20 vol % Composites.

4.9 Microstructure of Indented Samples of Alumina-YAG Composites.

Fig 4.15 (a-d) show the crack paths as observed in the FESEM on the indented samples of Alumina and Alumina-Yttrium Aluminate composites. Fig 4.15 (a) shows the crack path in a pure Alumina sample while Fig 4.15 (b, c, and d) show the crack path of Alumina– 20 vol% Yttrium Aluminate samples prepared from 40, 50 and 60 mol% Y_2O_3 addition to Alumina respectively. The microstructures show that the crack path in pure Alumina sample is relatively straight with only little deviation from the original crack path during its growth. On the other hand, the crack paths of all the Alumina-Yttrium Aluminate samples show a very tortuous crack path. In one or two cases, the crack path has formed a semi-circular path.

The deviation in the crack path or the crack bowing phenomenon indicates that in Alumina-Yttrium Aluminate samples the crack propagation becomes difficult, and the crack has to traverse a longer path for its progress or growth. This type of features indicates that the fracture toughness of the composites is expected to increase with Yttrium Aluminate addition in

Alumina. However, its potential can only be realized if the samples could be densified properly.

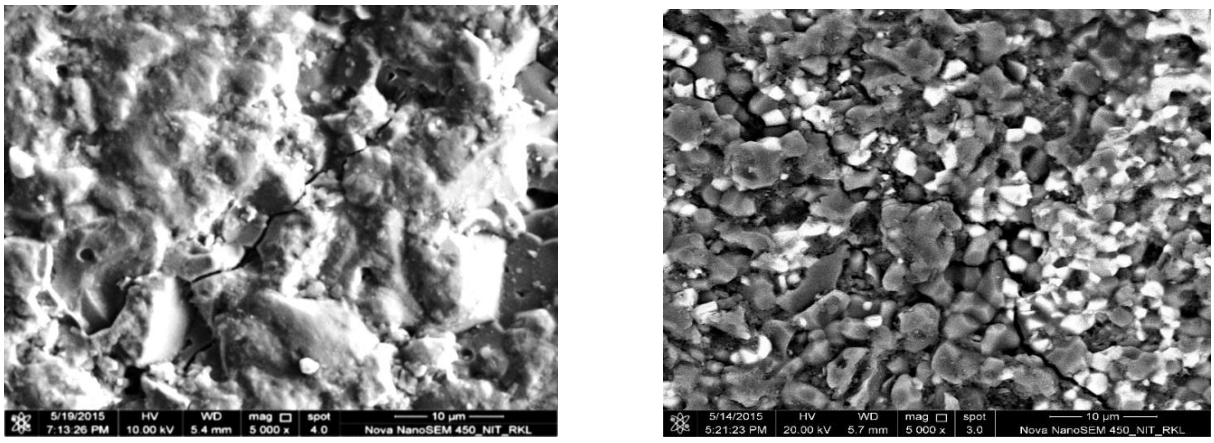

Fig- 4.15:-Crack path in the indented samples (a) Pure Alumina, (b) Alumina- 20 vol% YA (40 mol%).

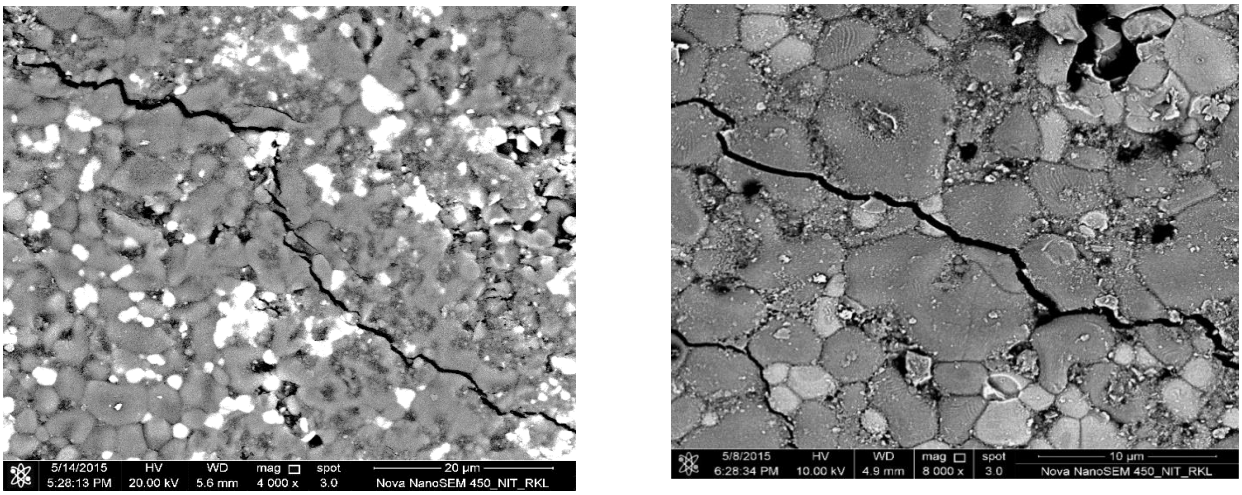

Fig- 4.16: -Crack path in the indented samples (a) Alumina- 20 vol% YA (50 mol%), (b) Alumina- 20 vol% YA (60 mol%).

Chapter-5

Conclusions

Alumina-Yttrium Aluminate composite was prepared by mixing Yttrium nitrate with calcined alumina. The mixed powder was dried at 60^{o}C and calcined at 1400^{o}C. The DSC indicate that the exothermic peaks at 900^{o}C to 1150^{o}C refer to the Yttrium Aluminate phase formation. The calcined powder was pressed and sintered at 1650^{o}C. The sintered samples were characterized by Relative Density, Apparent Porosity, Hardness, Fracture Strength, Fracture Toughness and Microstructure. Relative density, Hardness, 3 point Flexural strength & Fracture Toughness was highest for the composite with 15 vol % Yttrium Aluminate phase in Alumina. The increase in fracture toughness was correlated with the addition of YAG phase in Alumina which resulted in the increasing crack path length giving a crack bowing effect.

References

[1] P. Hing, and W. G. Groves, "The microstructure and fracture properties of MgO crystals containing a dispersed phase", Journal of Material Science, 1972, 7, 422-426.

[2] F. Kern, "Mechanical Properties and Microstructure of Y_2Nd-TZP/20 vol % Alumina Nanocomposites", Materialyceramiczne/Ceramic Material, 2012, 4(2), 165-171.

[3] K. Vishista, F. D. Gnanam, "Effect of Strontia on the densification and mechanical properties of sol–gel alumina", Ceramics International., 2006, 32, 917–922.

[4] R. A Cutler, R. J. Mayhew, K. M. Prettyman & A .V. Virkar,"High-toughness Ce-TZP/Al_2O_3 ceramics with improved hardness and strength", Journal of America Ceramics Society, 74(1): 179-186.

[5] R. Lach, K. Haberko, M. M. Bucko, M. Szumera, G. Grabowski, "Ceramic matrix composites in the alumina/5–30 vol. %YAG system", Journal of the European Ceramic Society, 2011, 31, 1889–1895.

[6] R. P. Rana, "Powder Processing, densification behaviour, microstructure and mechanical property of Al_2O_3-50 vol% ZrO_2 Composites", e-thesis NIT Rourkela, November -2009.

[7] M. Medraj, R. Hammond, M. A. Parvez, R. A. L. Drew, W. T. Thompson,"High-temperature neutron diffraction study of the Al_2O_3–Y_2O_3 system", Journal of the European Ceramic Society ,2006, 26, 3515–3524.

[8] Eduardo De Souza Lima, Luis Henrique, Leme Louro, Ricardo de Freitas, Cabral, Jose B. de Camposc, Roberto Ribeiro de Avillezd, Célio Albano da Costae,"Processing and Characterization of Al_2O_3-yttrium aluminium garnet powders", Journal of Materials Research and Technology ,2013, 2(1), 18-23.

[9] Tomoya Nagira and Hideyuki Yasuda, "Fabrication of Al_2O_3 YAG Equilibrium Eutectic Composites via Transformation from Fine Al_2O_3 and YAP Powder Mixtures" Materials Transactions, 2012, 53, 1124 -1129.

[10] Radosław Lach, Krzysztof Haberko, Mirosław Bućko "Synthesis of alumina/YAG 20 Vol % composite by co-precipitation", Processing and Application of Ceramics, 2011, 5, 187–189.

[11] R. Voytovych, I. MacLaren, M. A. Gulgun, R. M. Cannon, M. Ruhle, "The effect of Yttrium on densification and grain growth in α-alumina". Acta Materials, 2002, 50, 3453–3463.

[12] F. Sommer, F. Kern, H.F. E. Maghraby, M. Abou El-Ezz, M. Awaad, R. Gadow, S.M. Naga "Effect of preparation route on the properties of slip-casted Al_2O_3/YAG composites", Ceramics International, 2012,38, 4819-4826.

[13] Paola Palmero, Antonia Simone, Claude Esnouf, Gilbert Fantozzi, Laura Montanaro "Comparison among different sintering routes for preparing alumina-YAG nano-composites", Journal of the European Ceramic Society, 2006, 26, 941–947.

[14] Jose. Y. Pastor, Javier Llorcaw and Alicia Salazar "Mechanical Properties of Melt-Grown Alumina–Yttrium Aluminum Garnet Eutectics up to 1900 K". Journal of the American Ceramic Society, 2005, 1488–1495.

[15] P.Palmero, F.Lomello, G.Fantozzi, G.Bonnefont, "Alumina-YAG micro nano-composites: Elaboration and Mechanical Characterization", Materialyceramiczine /Ceramic Material/, 2010, 62, 533-539.

[16] H. B. Duong and J. Wolfenstine, "Creep behavior of fine-grained two-phase A1203-$Y_3A1_50_{12}$ materials", Materials Science and Engineering, 1993, 172, 173-179.

[17] S. Ochiai, T. Ueda, K. Sato, M. Hojo, Y. Waku, N. Nakagawa, S. Sakata, A. Mitani, T. Takahashi "Deformation and fracture behavior of an Al_2O_3/YAG composite from room temperature to 2023 K", Composites Science and Technology ,2001, 61, 2117–2128.

[18] Y. Waku, N. Nakagawa, T. Wakamoto, H. Ohtsubo, K. Shimizu, Y. Kohtoku, "High-temperature strength and thermal stability of a unidirectionally solidified Al2O3/YAG eutectic composite". Journal of Materials Science, 1998, 33, 1217–1225.

[19] J. Ramırez-Rico, A. R. Pinto-Gomez, J. Martınez-Fernandez,A . R. deArellano-Lopez, P. B. Oliete , J .I . Pena , V. M . Orera,"High-temperature plastic behaviour of Al_2O_3–$Y_3Al_5O_{12}$ directionally solidified eutectics". Acta Materialia 2006, 54, 3107–3116.

[20] ASTM: C1327-99, Standard Test Method for Vickers Indentation Hardness of Advanced Ceramics, 1999, 1-8.

[21] ASTM C1161-90, Standard Test Method for Flexural Strength of Advanced Ceramics an Ambient Temperature, Annual book of ASTM Standards, Vol. 15.01. ASTM, 327-333 (1991).

[22] P. Chantikul, G. R. Anstis, B. R. Lawn and D. B. Marshall, "A critical evaluation of indentation techniques for measuring toughness: II, strength method". Journal of American Ceramic Society, 1981, 64, 539–543.

[23] P. Melnikov, V. A. Nascimento, L. Z. Z. Consolo, A. F. Silva "Mechanism of thermal decomposition of Yttrium Nitrate Hexahydrate, $Y(NO_3)_36H_2O$ and modelling of intermediate oxynitrates" Journal of Thermal Analysis and Calorimetry 2013, 111,115–119.